

Published in final edited form as:

*Nat Genet.* 2015 September ; 47(9): 987–995. doi:10.1038/ng.3373.

## Genome-wide meta-analysis identifies five new susceptibility loci for cutaneous malignant melanoma

*A full list of authors and affiliations appears at the end of the article.*

# These authors contributed equally to this work.

### Abstract

Thirteen common susceptibility loci have been reproducibly associated with cutaneous malignant melanoma (CMM). We report the results of an international two-stage meta-analysis of 11 genome-wide association studies (GWAS, five unpublished) of CMM and Stage two datasets, totaling 15,990 cases and 26,409 controls. Five loci not previously associated with CMM risk reached genome-wide significance ( $P < 5 \times 10^{-8}$ ) as did two previously-reported but un-replicated loci and all thirteen established loci. Novel SNPs fall within putative melanocyte regulatory elements, and bioinformatic and eQTL data highlight candidate genes including one involved in telomere biology.

---

Cutaneous malignant melanoma (CMM) primarily occurs in fair-skinned individuals; the major host risk factors for CMM include pigmentation phenotypes<sup>1-4</sup>, the number of melanocytic nevi<sup>5,6</sup> and a family history of melanoma<sup>7</sup>.

Six population-based genome-wide association studies (GWAS) of CMM have been published<sup>8-13</sup> identifying 12 regions that reach genome-wide significance. Some of these regions were already established melanoma risk loci, for example through candidate gene studies<sup>14</sup> (for review see<sup>15</sup>). A 13<sup>th</sup> region in 1q42.12, tagged by rs3219090 in *PARP1*, that was borderline in the initial publication ( $P = 9.3 \times 10^{-8}$ )<sup>12</sup> was confirmed as genome-wide significant by a recent study ( $P = 1.03 \times 10^{-8}$ )<sup>16</sup>. As might be expected for common variants influencing CMM risk many of these loci contain genes that are implicated in one of the two

---

Users may view, print, copy, and download text and data-mine the content in such documents, for the purposes of academic research, subject always to the full Conditions of use:[http://www.nature.com/authors/editorial\\_policies/license.html#terms](http://www.nature.com/authors/editorial_policies/license.html#terms)

**Correspondence:** Correspondence should be addressed to Matthew H. Law ([matthew.law@qimrberghofer.edu.au](mailto:matthew.law@qimrberghofer.edu.au)) and Mark M. Iles ([M.M.Iles@leeds.ac.uk](mailto:M.M.Iles@leeds.ac.uk)).

<sup>35</sup>A full list of members and affiliations appears in the Supplementary Note.

<sup>67</sup>These authors jointly supervised this work

### Competing financial interests

The authors declare no competing financial interests

### URLs

GenoMEL, <http://www.genomel.org/>; Wellcome Trust Case Control Consortium <http://www.wtccc.org.uk/>; RegulomeDB, <http://RegulomeDB.org/>; HaploReg <http://www.broadinstitute.org/mammals/haploreg/>; GTEx <http://www.gtexportal.org>, MuTHER <http://www.muther.ac.uk/>, eQTL data accessed via GeneVAR <http://www.sanger.ac.uk/resources/software/genevar/>, eQTL Browser <http://eqtl.uchicago.edu/cgi-bin/gbrowse/eqtl/>; NHGRI GWAS catalog: <http://www.genome.gov/gwastudies/>; Genome-wide Complex Trait Analysis (GCTA) <http://www.complextaitgenomics.com/software/gcta/>; GTOOL <http://www.well.ox.ac.uk/~cfreeman/software/gwas/gtool.html>; Cancer Oncological Gene-environment Study <http://www.nature.com/icogs/primer/common-variation-and-heritability-estimates-for-breast-ovarian-and-prostate-cancers/#70>; VCFtools <http://vcftools.sourceforge.net/>; R scripts for Manhattan and QQ plots <http://gettinggeneticsdone.blogspot.com.au/2011/04/annotated-manhattan-plots-and-qq-plots.html>.

well-established heritable risk phenotypes for melanoma, pigmentation (*SLC45A2*, *TYR*, *MC1R* and *ASIP*) and nevus count (*CDKN2A/MTAP*, *PLA2G6* and *TERT*) (Supplementary Table 1)<sup>17</sup>. The presence of DNA repair genes such as *PARP1* and *ATM* at two loci suggests a role for DNA maintenance pathways, leaving four loci where the functional mechanism is less clear (*ARNT/SETDB1*, *CASP8*, *FTO* and *MX2*).

Of particular interest is *TERT*, which is involved in telomere maintenance; SNPs in this region have been associated with a variety of cancers<sup>11,18-22</sup>. Further, *ATM* and *PARP1*'s DNA repair functions extend to telomere maintenance and response to telomere damage<sup>23,24</sup>. Longer telomeres have been associated with higher nevus counts and it has been proposed that longer telomeres delay the onset of cell senescence, allowing further time for mutations leading to malignancy to occur<sup>20,25</sup>. There is evidence that longer telomeres increase melanoma risk<sup>20,26,27</sup> and that other telomere-related genes are likely involved in the etiology of melanoma, but none of these loci has yet reached genome-wide significance (or even  $P < 10^{-6}$ )<sup>28</sup>.

In addition, two independent SNPs at 11q13.3, near *CCND1*, and 15q13.1, adjacent to the pigmentation gene *OCA2*, have been associated previously with melanoma, but did not meet the strict requirements for genome-wide significance, either not reaching  $P = 5 \times 10^{-8}$  in the initial report, or not replicating in additional studies<sup>10,11,29</sup>. This meta-analysis has resolved the status of these two loci, as well as identified novel melanoma susceptibility loci.

## Results and Discussion

We conducted a two-stage genome-wide meta-analysis. Stage one consisted of 11 GWAS totaling 12,874 cases and 23,203 controls from Europe, Australia and the USA; this includes all six published CMM GWAS and five unpublished ones (Supplementary Table 2). In Stage two we genotyped 3,116 CMM cases and 3,206 controls from three additional datasets (consisting of 1,692 cases and 1,592 controls from Cambridge, UK, 639 cases and 823 controls from Breakthrough Generations, UK, and 785 cases and 791 controls from Athens, Greece; Online Methods) for the most significant SNP from each region reaching  $P < 10^{-6}$  and included these results in an Overall meta-analysis of both stages, totaling 15,990 melanoma cases and 26,409 controls. Details of these studies can be found in Supplementary Note. Given that the previous single-largest melanoma GWAS was of 2,804 cases and 7,618 controls<sup>11</sup>, this meta-analysis represents a fourfold increase in sample size compared to previous efforts to identify the genetic determinants of melanoma risk. Unless otherwise indicated we report the  $P$ -values from the Overall meta-analysis combining the two stages (Supplementary Table 3).

All Stage one studies underwent similar quality control (QC) procedures, were imputed using the same reference panel and the results analyzed in the same way, with the exception of the Harvard and MDACC studies (see Online Methods). A fixed effects ( $P_{fixed}$ ) or random effects ( $P_{random}$ ) meta-analysis was conducted as appropriate depending on between-study heterogeneity. 9,470,333 imputed variants passed QC in at least two studies, of which 3,253 reached  $P_{fixed} < 1 \times 10^{-6}$  and 2,543 reached  $P_{fixed} < 5 \times 10^{-8}$ . For reference we provide a list of SNPs that reached a  $P_{fixed}$ , or  $P_{random}$  if  $I^2 > 31\%$ , value  $< 1 \times 10^{-7}$

(Supplementary Table 4). The Stage one meta-analysis genome-wide inflation value ( $\lambda$ ) was 1.032, and as  $\lambda$  increases with sample size we also adjusted the  $\lambda$  to a population of 1,000 cases and 1,000 controls<sup>30</sup>. The resulting  $\lambda_{1000}$  of 1.002 suggested minimal inflation. Quantile-quantile (QQ) plots for the Stage one meta-analysis and individual GWAS studies can be found in Supplementary Figures 2 and 3. To further confirm that our results were not influenced by inflation, the Stage one meta-analysis was repeated correcting for individual studies'  $\lambda$ ;  $P$ -values were essentially unchanged (Online Methods, Supplementary Table 3).

All 13 previously-reported genome-wide significant loci (most first identified in one of the studies included here) reached  $P < 5 \times 10^{-8}$  in Stage one (Figure 1, Supplementary Table 4). In addition to confirming the two previously-reported sub-genome-wide significant loci at 11q13.3 (rs498136, 89 kb from *CCND1*) and 15q13.1 (rs4778138 in *OCA2*) we found three novel loci reaching genome-wide significance at 6p22.3, 7p21.1, and 9q31.2 (Table 1; Figure 2). Forest plots of the individual GWAS study results can be found in Supplementary Figure 1. SNPs in another 11 regions reached  $P < 10^{-6}$  (Supplementary Table 3); notably, three were close to known telomere-related genes (rs2995264 is in *OBFC1*<sup>31</sup> in 10q24.33, rs11779437 is 1.1 Mb from *TERF1*<sup>32</sup> in 8q13.3, and rs4731207 is 66 kb from *POT1* in 7q31.33, in which loss-of-function variants occur in some melanoma families<sup>33,34</sup>). Given the importance of telomeres in melanoma we additionally genotyped two SNPs that did not quite reach our  $P < 10^{-6}$  threshold but are close to telomere-related genes<sup>35</sup>: rs12696304 in 3q26.2 ( $P_{\text{fixed}} = 1.6 \times 10^{-5}$ ) is 1.1 kb from *TERC* and rs75691080 in 20q13.33 ( $P_{\text{fixed}} = 1.0 \times 10^{-6}$ ) is 19.4 kb from *RTEL1*. In total 18 SNPs were carried through to Stage two (Online methods).

Including the Stage two results in the Overall meta-analysis led to two new genome-wide significant regions, 2p22.2 and 10q24.33 (Figure 2; Table 1, Supplementary Table 3). The Stage two data also serve the purpose of independently confirming with genotype data the meta-analysis results from imputed SNPs. Five SNPs, rs4778138 (*OCA2*/15q13.1), rs498136 (*CCND1*/11q13.3), and the novel rs10739221 (9q31.2), rs6750047 (2p22.2) and rs2995264 (10q24.33) all reached  $P < 0.05$  in the genotyped Stage two samples. We have estimated the power to reach  $P < 0.05$  in the Stage two samples for all SNPs that reached genome-wide significance in the Stage one meta-analysis (Online Methods, Supplementary Table 5). rs6914598 (6p22.3) was only genotyped in the Athens sample and thus had a power of only 0.35. Of the remaining four SNPs that were genome-wide significant in Stage one, while the 7p21.1 SNP rs1636744 was well powered ( $> 90\%$ ), the probability that all four of these well-powered SNPs would reach  $P < 0.05$  in the analysis of Stage two data was only  $(0.916 \times 0.736 \times 0.787 \times 0.955) = 0.51$ , so it is not surprising that one was not significant. The SNPs in 7p21.1 (rs1636744) and 6p22.3 (rs6914598) did not reach nominal significance in Stage two, but for both SNPs the confidence intervals for the effect estimates overlapped those from the Stage one meta-analysis.

In terms of heritability the 13 loci that were genome-wide significant before this meta-analysis explained 16.9% of the familial relative risk (FRR) for CMM, with *MC1R* explaining 5.3% alone (Online Methods). Including the seven loci confirmed or reported here (2p22.2, 6p22.3, 7p21.1, 9q31.2, 10q24.33, 11q13.3, 15q13.1), an additional 2.3% of

FRR is explained. In total, all 20 loci explain 19.2% of the FRR for CMM; this is a conservative estimate given the assumption of a single SNP per locus.

We tested all new and known CMM risk loci for association with nevus count or pigmentation (Supplementary Table 1). Aside from the known association between *OCA2* and pigmentation, none of the newly-identified loci were associated ( $P > 0.05$ ). Following confirmation of the loci in the Stage two analysis, we performed conditional analysis on the Stage one meta-analysis results to determine whether there were additional association signals within 1 Mb either side of the top SNP at each locus using the Genome-wide Complex Trait Analysis (GCTA) software<sup>36</sup>(Online Methods; Supplementary Table 6). This indicated that while there are additional SNPs associated with CMM at each locus, for all but chromosome 7 and 11 the additional signals were not strongly associated with melanoma ( $P < 1 \times 10^{-7}$ ; for more detail see Supplementary Note). We then conducted a comprehensive bioinformatic assessment of the top SNP from each of the seven new genome-wide significant loci using a range of annotation tools, databases of functional and eQTL results and previously-published GWAS results (see Online Methods, Supplementary Tables 7–9). We applied the same analyses to each locus but, to limit repetition, where nothing was found for a given resource (e.g. NHGRI GWAS catalog) we do not explicitly report this.

## 2p22.2

While rs6750047 in 2p22.2 was not genome-wide significant in the Stage one meta-analysis it reached genome-wide significance ( $P_{fixed} = 7.0 \times 10^{-9}$ , OR = 1.10,  $I^2 = 0.00$ ; Table 1, Supplementary Table 3) in the Stage two and Overall meta-analysis. The association signals for 2p22.2 (Figure 2) span the 3' UTR of *RMDN2* (also known as *FAM82A1*) and the entirety of the *CYP1B1* gene, and as such there is a wealth of bioinformatic annotation for SNPs associated with CMM risk. Considering the 26 SNPs with  $P$ -values within two orders of magnitude of rs6750047 in 2p22.2 (Supplementary Tables 7–9), HaploReg<sup>37</sup> reports a significant enrichment of strong enhancers in epidermal keratinocytes (4 observed, 0.6 expected,  $P = 0.003$ ). The paired rs162329 and rs162330 (LD  $r^2 = 1.0$ , 98 bp apart;  $P_{fixed} = 3.91 \times 10^{-6}$ ,  $I^2 = 11.23$ ) lie approximately 10 kb upstream from the *CYP1B1* transcription start site in a potential enhancer in keratinocytes and other cell types<sup>37-40</sup>. These two SNPs are eQTLs for *CYP1B1* in three independent liver sample sets<sup>41,42</sup>. In addition several SNPs, including the peak SNP for 2p22.2, rs6750047, are strong *CYP1B1* eQTLs in LCLs in the Multiple Tissue Human Expression Resource<sup>43</sup> (MuTHER;  $P < 5 \times 10^{-5}$ ). It is worth noting the overlap between the liver and lymphoblastoid cell line (LCL) eQTLs is incomplete; rs162330 and rs162331 are only weak eQTLs in MuTHER data ( $P \sim 0.01$ ). In terms of functional annotation the most promising SNP near rs6750047 is rs1374191 ( $P_{fixed} = 5.4 \times 10^{-5}$ , OR = 1.07,  $I^2 = 0.00$ ); in addition to being a *CYP1B1* eQTL in LCLs (MuTHER  $P = 6.9 \times 10^{-8}$ ); this SNP is positioned in a strong enhancer region in multiple cell types including melanocytes and keratinocytes<sup>37-40</sup>. In summary, SNPs in 2p22.2 associated with melanoma lie in putative melanocyte and keratinocyte enhancers and are also cross-tissue eQTLs for *CYP1B1*.

*CYP1B1* metabolizes endogenous hormones, playing a role in hormone associated cancers including breast and prostate (reviewed in<sup>44</sup>). *CYP1B1* also metabolizes exogenous chemicals, resulting in pro-cancer (e.g. polycyclic aromatic hydrocarbons) and anti-cancer (e.g. tamoxifen) outcomes<sup>44</sup>. The former is of interest as *CYP1B1* is regulated by *ARNT*, a gene at the melanoma-associated 1q21 locus<sup>12</sup>. The *CYP1B1* promoter is methylated in melanoma cell lines and tumor samples<sup>45</sup>. *CYP1B1* missense protein variants have been associated with cancers including squamous cell carcinoma and hormone associated cancers<sup>44,46</sup>. Of these only rs1800440 (p.Asn453Ser) is moderately associated with melanoma ( $P_{fixed} = 1.83 \times 10^{-5}$ , OR = 0.90,  $I^2 = 0.00$ ), and it was included in the bioinformatic annotation (Supplementary Tables 7–9). rs1800440 is not in LD with the CMM risk meta-analysis peak SNP rs6750047/2p22.2 (LD  $r^2 = 0.04$ ) and adjusting for rs6750047 only slightly reduces its association with CMM ( $P = 4.3 \times 10^{-4}$ , Online Methods). Truncating mutations in *CYP1B1* are implicated in primary congenital glaucoma<sup>47</sup> and since glaucoma cases are used as controls in the contributing WAMHS melanoma GWAS, we considered the impact of excluding glaucoma cases; the SNP remains genome-wide significantly associated with CMM even after such exclusions (Supplementary Note, Supplementary Table 10). While the association with melanoma in the WAMHS set is stronger without glaucoma cases (beta 0.05 vs. 0.19) both betas are within the range observed for other melanoma datasets and no heterogeneity ( $I^2 = 0.00$ ) is observed with or without the glaucoma samples.

### 6p22.3

rs6914598 ( $P_{fixed} = 3.5 \times 10^{-8}$ , OR = 1.11,  $I^2 = 0.00$ ) lies in 6p22.3, in intron 12 of *CDKALI*, a gene that modulates the expression of a range of genes including proinsulin via tRNA methylthiolation<sup>48,49</sup>. Bioinformatic assessment of the 35 SNPs with  $P$ -values within two orders of magnitude of the 6p22.3 peak rs6914598 by HaploReg<sup>37</sup> indicates that the most functionally interesting SNP is rs7776158 (Stage one  $P_{fixed} = 3.8 \times 10^{-8}$ ,  $I^2 = 0$ , in complete LD with rs6914598,  $r^2 = 1.0$ ), which lies in a predicted melanocyte enhancer that binds IRF4<sup>38,39</sup>. IRF4 binding is of interest given the existence of a functional SNP rs12203592 in the *IRF4* gene<sup>50</sup>, associated with nevus count, skin pigmentation and tanning response<sup>51-54</sup>.

### 7p21.1

rs1636744 ( $P_{fixed} = 7.1 \times 10^{-9}$ , OR = 1.10,  $I^2 = 0.00$ ; Figure 2) is in an intergenic region of 7p21.1 and lies 63 kb from *AGR3*. rs1636744 is an eQTL for *AGR3* in lung tissue (GTEx  $P = 1.6 \times 10^{-6}$ )<sup>55,56</sup>. *AGR3* is a member of the protein disulphide isomerase family, which generate and modify disulphide bonds during protein folding<sup>57</sup>. *AGR3* expression has been associated with breast cancer risk<sup>58</sup> and poor survival in ovarian cancer<sup>59</sup>. GTEx confirms that *AGR3* is expressed in human skin samples. Evidence that the regions containing rs1636744 are not conserved in primates (UCSC genome browser<sup>60</sup>), and RegulomeDB<sup>40</sup> indicates there is little functional activity at this SNP. More promising are rs847377 and rs847404 which, in addition to being both *AGR3* eQTLs in lung tissue<sup>55</sup> and associated with CMM risk (Stage one  $P_{fixed} = 3.89 \times 10^{-8}$  and  $1.72 \times 10^{-7}$ ), are in putative weak enhancers in a range of cells including melanocytes and keratinocytes<sup>37-40</sup>. Adjusting for rs1636744

renders rs847377 and rs847404 non-significant ( $P > 0.6$ ) indicating that they are tagging a common signal. rs1636744, rs847377 and rs847404 are not eQTLs for *AGR3* in sun-exposed skin.

### 9q31.2

The melanoma-associated variants at 9q31.2, peaking at rs10739221 (Overall  $P_{fixed} = 7.1 \times 10^{-11}$ ;  $I^2 = 0.00$ ; Figure 2) are intergenic. The nearest genes are *TMEM38B*, *ZNF462* and the nucleotide excision repair gene *RAD23B*<sup>61</sup>. While bioinformatic annotation did not reveal any putative functional SNPs, based on the importance of DNA repair in melanoma, *RAD23B* is of particular interest. rs10739221 is 635 Kb from the leukemia-associated *TAL2*<sup>62</sup>, and 1.2 Mb from *KLF4*, which regulates both telomerase activity<sup>63</sup> and the melanoma-associated *TERT*<sup>64</sup>.

### 10q24.33

While not genome-wide significant in Stage one, rs2995264 in 10q24.33 is strongly associated with telomere length<sup>28,35</sup> and was genotyped in Stage two. rs2995264 was significantly associated with CMM in the Cambridge study ( $P = 0.046$ ) and strong in the Breakthrough dataset ( $P = 8.0 \times 10^{-4}$ ); in the Overall meta-analysis this SNP reached genome-wide significance ( $P_{fixed} = 2.2 \times 10^{-9}$ ;  $I^2 = 27.14$ ). The melanoma association signal at 10q24.33 (Figure 2) spans the *OBFC1* gene and the promotor of *SH3PXD2A*. Given the strong telomere length association at this locus the most promising candidate is *OBFC1*, a component of the telomere maintenance complex<sup>31</sup>.

HaploReg reports that SNPs within two orders of magnitude of rs2995264 in 10q24.33 are significantly more likely to fall in putative enhancers in keratinocytes than would be expected by chance. Promising candidate functional SNPs include the conserved rs11594668 and rs11191827 which lie in putative melanocyte and keratinocyte enhancers, and bind transcription factors<sup>37-40</sup>. The association observed at rs2995264/10q24.33 is independent of a recent report of a melanoma association at 10q25.1<sup>65</sup>. Our peak SNP for 10q24.33, rs2995264, and the 10q25.1 SNPs rs17119434, rs17119461, and rs17119490 reported in Teerlink et al., (2012)<sup>65</sup> are in linkage equilibrium (LD  $r^2 < 0.01$ ) and in turn these SNPs are not associated with CMM in our meta-analysis ( $P > 0.2$ ).

### 11q13.3

The CMM-associated variants at 11q13.3 peak at rs498136 (Overall  $P_{fixed} = 1.5 \times 10^{-12}$ , OR = 1.13,  $I^2 = 0.00$ ; Supplementary Figure 4) 5' to the promotor of *CCND1*. In the initial report of *CCND1*<sup>11</sup> rs11263498 was borderline in its association with melanoma ( $P = 3.2 \times 10^{-7}$ ) and while supported ( $P = 0.017$ ) by the two replication studies exhibited significant heterogeneity and did not reach genome-wide significance (overall  $P_{random} = 4.6 \times 10^{-4}$ ,  $I^2 = 45.00$ ). The previously-reported rs11263498 and the meta-analysis peak of rs498136/11q13.3 are in strong linkage disequilibrium (LD) ( $r^2 = 0.95$ ).

Bioinformatic assessment of the *CCND1* region indicated the peak SNP rs498136/11q13.3 is in a putative enhancer in keratinocytes in both ENCODE and Roadmap data<sup>37-40</sup>.

Considering other SNPs strongly associated with CMM, both the previously-reported<sup>11</sup> rs11263498 (Stage one  $P_{fixed} = 1.8 \times 10^{-9}$ , OR = 1.12,  $I^2 = 0.00$ ) and rs868089 (Stage one  $P_{fixed} = 2.0 \times 10^{-9}$ , OR = 1.12,  $I^2 = 0.00$ ) lie in putative melanocyte enhancers.

Somatic *CCND1* amplification in CMM tumors positively correlates with markers of reduced overall survival, including Breslow thickness and ulceration<sup>66,67</sup>. The *CCND1* association with breast cancer has been extensively fine-mapped, revealing three independent association signals<sup>68</sup>. rs554219 and rs75915166 tag the two strongest functional associations with breast cancer<sup>68</sup> but are not themselves associated with CMM risk (Stage one  $P_{fixed} > 0.1$ ,  $I^2 = 0.00$ ). While the third signal in breast cancer was not functionally characterized<sup>68</sup>, its tag SNP rs494406 is modestly associated with CMM (Stage one  $P_{fixed} > 0.0002$ ,  $I^2 = 0.00$ , LD  $r^2=0.47$  with rs498136/11q13.3). rs494406 is no longer significant after adjustment by rs498136 ( $P = 0.53$ ; Supplementary Table 6), suggesting that SNPs that are in LD in this region are associated with risk of both melanoma and breast cancer.

## 15q13.1

Both *OCA2* and nearby *HERC2* at the 15q13.1 locus have long been associated with pigmentation traits<sup>51</sup>. rs12913832 in *HERC2*, also known as rs11855019, is the major determinant of eye color in Europeans<sup>69</sup>, making this region a strong candidate for CMM risk. One of the studies contributing to this meta-analysis previously reported a genome-wide significant association between melanoma and rs1129038 and rs12913832 in *HERC2* (in strong LD<sup>10</sup> reported as  $r^2 = 0.985$ ), but this was not supported ( $P > 0.05$ ) by any of the three replication GWAS (final  $P = 2.5 \times 10^{-4}$ )<sup>10</sup>. Stratification might be an issue for this locus as eye color frequencies vary markedly across European populations. Indeed, in our meta-analysis, which includes all four of these GWAS, both rs1129038 and rs12913832 showed highly heterogeneous effects in the CMM risk meta-analysis ( $P_{random} = 0.037$  and 0.075 respectively,  $I^2 > 77.00$ ).

Amos et al., (2011) found that rs4778138 in *OCA2*, which is only in weak LD with rs12913832 ( $r^2 = 0.12$ ), exhibited a more consistent association across studies, albeit not genome-wide significantly. In our Overall meta-analysis we confirm rs4778138 in 15q13.1 is associated with CMM risk ( $P_{fixed} = 2.2 \times 10^{-11}$ , OR = 0.84,  $I^2 = 0.00$ ; Figure 2). Following adjustment of the 15q13.1 signal by rs4778138 the effect size for the eye color SNP rs12913832 is reduced from beta = 0.12 to beta = 0.064. Conversely adjustment for rs12913832 reduces rs4778138's association with CMM (beta reduced from -0.178 to -0.114, corrected  $P = 1.6 \times 10^{-4}$ ). rs12913832 is poorly imputed across studies, reaching INFO > 0.8 in only 6 studies, and we are unable to conclusively exclude a role for rs12913832 at this locus. HaploReg indicates rs4778138 is within a putative melanocyte enhancer in Roadmap epigenetic data<sup>37-40</sup>. While it is not clear which gene(s) in 15q13.1 is/are influenced by melanoma-associated SNPs, the fact that rs4778138 is associated with eye colors intermediate to blue and brown<sup>70</sup> supports a role for *OCA2*.

## Evidence of additional melanoma susceptibility loci

A further nine loci were associated with CMM risk at multiple SNPs with  $P < 10^{-6}$  in Stage one but did not reach  $P < 5 \times 10^{-8}$  in the Overall meta-analysis (Supplementary Table 3).

Given that genome-wide significance is based on a Bonferroni correction assuming 1,000,000 independent tests, we would expect only one locus to reach  $P < 10^{-6}$  and the probability that as many as nine loci reach this threshold is  $1.1 \times 10^{-6}$  (exact binomial probability), so it is highly likely that several of these are genuine.

Of the 16 regions that reached  $P < 10^{-6}$ , three were near genes involved in telomere biology 7q31.33 (rs4731207 near *POT1*), 8q13.3 (rs11779437 near *TERF1*), and 10q24.33 (rs2995264 near *OBFC1*) (Supplementary Table 3). Given the evidence for telomere biology in melanoma<sup>20,25-28</sup> and that previous genome-wide significant SNPs are near the telomere maintenance genes *TERT*, *PARP1* and *ATM*, we included two further biological candidates: rs12696304, 1.1 kb from *TERC* in 3q26.2, and rs75691080 in 20q13.33 near *RTEL1*. Of these five SNPs, rs2995264 (10q24.33/*OBFC1*) attained genome-wide significance in the overall analysis while rs12696304 (3q26.2/*TERC*) was significant in Stage two ( $P = 4.0 \times 10^{-3}$ ), and reached  $P = 2.8 \times 10^{-7}$  in the Overall meta-analysis (Supplementary Table 3). While falling short of genome-wide significance this is nonetheless suggestive of an association at this locus. Neither rs4731207 (66 kb from *POT1* in 7q31.33) nor rs75691080 (19.4 kb from *RTEL1* in 20q13.33) were significantly associated with melanoma risk in Stage two, but in neither case did the estimated effect differ significantly from Stage one. In addition rs75691080 (*RTEL1*/20q13.33) is marginally associated with nevus count ( $P = 0.058$ ; Supplementary Table 1). Of the SNPs near telomere-related genes, rs11779437 in 8q13.3 was the most distant (1.1 Mb from *TERF1*) and was the only one to show a significantly different effect in Stage two (Overall  $P_{random} = 0.013$ , OR = 0.93,  $I^2 = 42.06$ ). This is most likely due to the initial signal being a false positive, but may be due to a lack of power.

## Conclusion

This two-stage meta-analysis, representing a fourfold increase in sample size compared to the previous largest single melanoma GWAS, has confirmed all thirteen previously reported loci, as well as resolving two likely associations at *CCND1* and *HERC2/OCA2*. The *CCND1* association with melanoma only partially overlaps the signal observed for breast cancer<sup>68</sup>. The *HERC2/OCA2* association is with rs4778138/15q13.1, which may be a subtle modifier of eye color<sup>70</sup>, but we cannot rule out that the association at this locus is influenced by the canonical blue/brown eye color variant rs12913832.

Our Stage one meta-analysis of over 12,000 melanoma cases identified three novel risk regions, with only rs10739221 formally significant ( $P < 0.05$ ) in Stage two (Table 1). Two further loci (2p22.2 and 10q24.33) reached genome-wide significance with the addition of the Stage two data (Figure 2; Table 1, Supplementary Table 3). In total our Overall meta-analysis identified 20 genome-wide significant loci; 13 previously replicated, two previously-reported but first confirmed here and five that are novel to this report. The new loci identified in this meta-analysis explain an additional 2.3% of the familial relative risk for CMM. Overall, 19.2% of the FRR is explained by all 20 genome-wide significant loci combined.



Except for the association at 9q31.2, the reported loci contain SNPs that are both strongly associated with melanoma and fall within putative regulatory elements in keratinocyte or melanocyte cells, with the nearby nucleotide excision repair gene *RAD23B* at 9q31.2 a promising candidate. eQTL datasets suggest that melanoma-associated SNPs at 7p21 regulate the expression of *AGR3* albeit in lung tissue and not sun-exposed skin. *AGR3* expression has been implicated in breast and ovarian cancer outcome. SNPs in 2p22.3 are associated with the expression of *CYP11B1*. Although this gene is better known for its role in hormone-associated cancers it may influence melanoma risk through metabolism of exogenous compounds, a process regulated by *ARNT* at the 1q21 melanoma-associated locus.

We have used the power of this large collection of CMM cases and controls to identify five novel loci, none of which are significantly associated with classical CMM risk factors and thus highlight novel disease pathways. Interestingly, we now have genome-wide significant evidence for association between CMM risk and a SNP in the telomere-related gene *OBFC1* in 10q24.33, in addition to the established telomere-related associations at the *TERT/CLPTMIL*, *PARP1* and *ATM* loci. We also have support, albeit not genome-wide significant, for *TERC*, the most significant predictor of leukocyte telomere length in a recent study<sup>35</sup>. Of the 20 loci that now reach genome-wide significance for CMM risk, five are in regions known to be related to pigmentation, three in nevus-related regions and four in regions related to telomere maintenance. This gives further evidence that the telomere pathway, with its effect on the growth and senescence of cells, may be important in understanding the development of melanoma.

## Online Methods

### Stage one array genotyping

The samples were genotyped on a variety of commercial arrays, detailed in the Supplementary Note.

### Stage one genome-wide imputation

Imputation was conducted genome-wide, separately on each study, following a shared protocol. SNPs with  $MAF < 0.03$  ( $MAF < 0.01$  in AMFS, Q-MEGA\_omni, Q-MEGA\_610k, WAMHS, and HEIDELBERG), control Hardy-Weinberg equilibrium (HWE)  $P < 10^{-4}$  or missingness  $> 0.03$  were excluded, as were any individuals with call rates  $< 0.97$ , identified as first degree relatives and/or European outliers by principal components analysis using Eigenstrat<sup>71</sup>. In addition, in each study where genotyping was conducted on more than one chip, any SNP not present on all chips was removed prior to imputation to avoid bias. IMPUTEv2.2<sup>72,73</sup> was used for imputation for all studies but Harvard, which used MaCH<sup>74,75</sup> and MDACC which used MaCH and minimac<sup>76</sup>. For GenoMEL, CIDRUK and MDACC samples the 1000 Genomes Feb 2012 data (build 37) was used as the reference panel, while for the AMFS, Q-MEGA\_omni, Q-MEGA\_610k, WAMHS, MELARISK and HEIDELBERG datasets the 1000 Genomes April 2012 data (build 37) was the reference for imputation<sup>77</sup>. In both cases any SNP with  $MAF < 0.001$  in European (CEU) samples was dropped from the reference panel. The HARVARD data were imputed using MACH with

the NCBI build 35 of phase II HapMap CEU data as the reference panel and only SNPs with imputation quality  $R^2 > 0.95$  were included in the final analysis.

### Stage one genome-wide association analysis

Imputed genotypes were analyzed as expected genotype counts based on posterior probabilities (gene dosage) using SNPTEST<sup>78</sup> assuming an additive model with geographic region as a covariate (SNPTEST v2.5 for chromosome X). MDACC imputed genotypes were analyzed using best guess genotypes from MACH and PLINK was used for logistic association test adjusting by the top two principle components. Only those with an imputation quality score (INFO/MaCH  $R^2$ ) score  $> 0.8$  were analyzed. Potential stratification was dealt with in the GenoMEL samples by including geographic region as a covariate (inclusion of principal components as covariates was previously found to make little difference<sup>9</sup>) and elsewhere by including principal components as covariates<sup>71</sup>.

### Meta-analysis

Heterogeneity of per-SNP effect sizes in studies contributing to the Stage one, Stage two and the Overall meta-analyses was assessed using the  $I^2$  metric<sup>79</sup>.  $I^2$  is commonly defined as the proportion of overall variance attributable to between-study variance, with values below 31% suggesting no more than mild heterogeneity. Where  $I^2$  was less than 31% a fixed effects model was used, with fixed effects  $P$ -values indicated by  $P_{\text{fixed}}$ ; otherwise random effects were applied ( $P_{\text{random}}$ ). The method of DerSimonian and Laird<sup>80</sup> was used to estimate the between-studies variance,  $\hat{\tau}^2$ . An overall random effects estimate was then calculated using the weights  $1 / (\nu_i + \hat{\tau}^2)$  where  $\nu_i$  is the variance of the estimated effect.  $\hat{\tau}^2 = 0$  for the fixed effects analyses. We report those loci reaching significance at  $> 1$  marker incorporating information from  $> 1$  study. Results for rs186133190 in 2p15 were only available from four studies; all other SNPs reported here utilize data from at least eight studies (Supplementary Table 3).

Per-study QQ plots of GWAS  $P$ -values are provided (Supplementary Figure 3) and for the Stage one meta-analysis (Supplementary Figure 3A). We also provide the Stage one QQ plot with previously reported regions removed (Supplementary Figure 2B). While there was minimal inflation remaining following PC/region of origin correction, to ensure residual genomic inflation was not biasing our results the meta-analysis was repeated using the genome-wide association meta-analysis software, GWAMA v2.1<sup>81</sup>. Included studies were corrected by inflating SNP variance estimates by their genomic inflation ( $\lambda$ ). As expected, given the low level of residual inflation, corrected and uncorrected results were very similar. GIF-corrected  $P$ -values are provided in Supplementary Table 3.

### Stage two genotyping

A single SNP for each of the 16 novel region reaching  $P < 10^{-6}$  in Stage one was subsequently genotyped in 3 additional melanoma case-control sets in Stage two (Supplementary Table 3). Any region that only showed evidence for association with CMM at a single imputed SNP and in only one study was not followed up. Included in the Stage two genotyping were rs75691080 in 20q13.33 which, while not quite reaching  $P < 10^{-6}$ , lies

20 kb from *RTEL1*; and rs12696304 in 3q26.2 which lies 1 kb from *TERC*. Both these genes are known to be telomere-related and have been associated with leukocyte telomere length<sup>35</sup>. The 16 novel regions included rs2290419 at 11q13.3 which is 450 kb away from our primary hit in the region of *CCND1* (rs498136, Supplementary Figure 4) and is in linkage equilibrium with the genome-wide significant hit in this region ( $r^2 = 0.002$ ) so may represent an independent effect.

The first Stage two dataset of 1,797 cases and 1,709 controls from two studies based in Cambridge, UK (see Supplementary Note for details of samples). These were genotyped using TaqMan® assays [Applied Biosystems]. 2 µl PCR reactions were performed in 384 well plates using 10 ng of DNA (dried), using 0.05 µl assay mix and 1 µl Universal Master Mix [Applied Biosystems] according to the manufacturer's instructions. End point reading of the genotypes was performed using an ABI 7900HT Real-time PCR system [Applied Biosystems].

The second was 711 cases and 890 controls from the Breakthrough Generations Study. These were genotyped in the same way as the Cambridge Stage two samples above.

The third was 800 cases and 800 controls from Athens, Greece. Genomic DNA was isolated from 200 µl peripheral blood using the QIAamp DNA blood mini kit [Qiagen]. DNA concentration was quantified in samples prior to genotyping by using Quant-iT dsDNA HS Assay kit [Invitrogen]. The concentration of the DNA was adjusted to 5 ng/µl. Selected SNPs were genotyped using the Sequenom iPLEX assay [Sequenom]. Allele detection in this assay was performed using matrix-assisted laser desorption/ionization –time-of-flight mass spectrometry<sup>82</sup>. Since genotyping was performed by Sequenom, specific reaction details are not available. As it is described by Gabriel et al.,<sup>82</sup> the assay consists of an initial locus-specific PCR reaction, followed by single base extension using mass-modified dideoxynucleotide terminators of an oligonucleotide primer which anneals immediately upstream of the polymorphic site of interest. Using MALDI-TOF mass spectrometry, the distinct mass of the extended primer identifies the SNP allele.

Genotyping of 18 SNPs was attempted in Stage two; the rs186133190/2p15. rs6750047/2p22.2, rs498136/11q13.3 and rs4731742/7q32.3 assays failed in one or more Stage two datasets (Supplementary Table 3). After QC (excluding individuals missing >1 genotype call, SNPs missing in > 3% of samples, SNPs with HWE  $P < 5 \times 10^{-4}$ ) there were 1,692 cases and 1,592 controls from Cambridge, 639 cases and 823 controls from Breakthrough Generations and 785 cases and 791 controls from Athens, Greece available for Stage two.

### Statistical power for Stage two

We have estimated the power to reach  $P < 0.05$  in the Stage two samples for all SNPs that reached genome-wide significance in the Stage one meta-analysis (Supplementary Table 3). We converted ORs to genotype relative risks (as the SNPs are relatively frequent this is a reasonable assumption) and estimated power by simulating cases and controls (10,000 iterations) and conducting a Cochran-Armitage trend test (see Supplementary Table 5).

## Conditional Analysis

Genome-wide Complex Trait Analysis (GCTA)<sup>36</sup> was used to perform conditional/joint GWAS analysis of newly identified or confirmed loci. GCTA allows conditional analysis of summary meta-analysis if provided with a sufficiently large reference population (2–5,000 samples) used in the meta-analysis to estimate LD. We used the QMEGA-610k set as a reference population to determine LD. QMEGA-610k imputation data for well imputed SNPs (INFO > 0.8) was converted to best guess genotypes using the GTOOL software (see URLs).

Following best-guess conversion (genotype probability threshold 0.5), SNPs with MAF < 0.01 and > 3% missingness were removed. As per Yang et al., (2011)<sup>36</sup> we further cleaned the QMEGA-610K dataset to include only completely unrelated individuals (Identity by descent score = 0.025 versus the standard 0.2 used in the meta-analysis), leaving a total of 4,437 people and 7.24 million autosomal SNPs in the reference panel.

Within each new locus, Stage one fixed effects summary meta-analysis data for SNPs within 1 Mb either side of the top SNP were adjusted for the top SNP using the --cojo-cond option. As per Yang et al., (2011) we used the genomic control corrected GWAS-meta-analysis results. Where there remained an additional SNP with  $P < 5 \times 10^{-8}$  following adjustment for the top SNP we performed an additional round including both SNPs. If the remaining SNPs had  $P$ -values greater than  $5 \times 10^{-8}$  no further analysis was performed. The results of this analysis are reported in Supplementary Table 6.

## Proportion of Familial Relative Risk

We have used the formula for calculating the proportion of familial relative risk (FRR) as outlined by the Cancer Oncological Gene-environment Study (see URLs). Given that CMM incidence is low, and the odds ratios reported small, we have assumed the odds ratios derived from the Stage one meta-analysis are equivalent to relative risks. With this assumption we have estimated the proportion of the FRR explained by each SNP ( $FRR_{\text{SNP}}$ ) as  $FRR_{\text{SNP}} = (pr^2 + q)/(pr + q)^2$

Where risk allele and alternative allele frequency are  $p$  and  $q$  respectively, and  $r$  is the odds ratio for the risk allele

Assuming a  $FRR_{\text{melanoma}}$  for CMM of 2.19<sup>83</sup> and using the combined effect of all SNPs (assuming a multiplicative effect and a single SNP per loci), we computed the proportion of FRR is explained by a set of SNPs as  $\log_e(\text{product of } FRR_{\text{SNP}}) / \log_e(FRR_{\text{melanoma}})$ .

## Association with nevus count or pigmentation

Pigmentation and nevus phenotype data were available for 980 melanoma cases and 499 control individuals from the Leeds case-control study<sup>84,85</sup>. Additional individuals from the Leeds melanoma cohort study<sup>86</sup> included pigmentation data giving a total of 1,458 subjects with melanoma and 499 control subjects. For the most significant SNP in each region reaching  $P < 1 \times 10^{-6}$  in the initial meta-analysis, logged age- and sex-adjusted total nevus count was regressed on the number of risk alleles, adjusting for case-control status. A sun-

sensitivity score was calculated for all subjects based on a factor analysis of six pigmentation variables (hair color, eye color, self-reported freckling as a child, propensity to burn, ability to tan and skin color on the inside upper arm)<sup>19</sup>. This score was similarly regressed on number of risk alleles and adjusted for case-control status. Full results can be found in Supplementary Table 1.

### Bioinformatic annotation

As the SNP most associated with the phenotype is quite likely not the underlying functional variant<sup>87</sup> at each locus we considered SNPs with  $P_{fixed}$  if  $I^2 < 31\%$ , or  $P_{random}$  if  $I^2 \geq 31\%$ , within a factor of 100 of the peak SNP for comprehensive bioinformatic assessment. To ensure we were not missing potentially interesting functional candidates, HaploReg was used to identify additional SNPs within 200kb and with LD  $r^2 > 0.8$  using 1000 Genomes pilot data<sup>37,77</sup>. GCTA was used to confirm that SNPs carried forward for bioinformatic assessment derived from a common signal. Following adjustment for the locus' top SNP, the SNPs selected for bioinformatic annotation at 6p22.3, 7p21.1, 10q24, 11q13.3 and 15q13.1 had CMM association  $P > 0.01$ . At 9q31.2 a single SNP rs1484384 retained a modest melanoma association ( $P = 0.008$ ) following adjustment for rs10739221; the rest were  $P > 0.01$ . At 2p22.2 those SNPs with  $P$ -values within 2 orders of magnitude of the peak SNP rs6750047 included rs1800440, a non-synonymous SNP with limited LD with rs6750047 (LD  $r^2 = 0.04$ ). Following adjustment for rs6750047, the significance of rs1800440 was essentially unchanged ( $P = 4.3 \times 10^{-4}$ ) and a second SNP rs163092 remained weakly associated with melanoma ( $P = 0.008$ ); all other SNPs had  $P > 0.01$ . Adjustment for both rs6750047 and rs1800440 removed the association between rs163092 and CMM ( $P > 0.01$ ).

HaploReg<sup>37</sup> and RegulomeDB<sup>40</sup> were crosschecked to explore data reflecting transcription factor binding, open chromatin and the presence of putative enhancers. These tools summarize and collate data from public databases ENCODE<sup>39</sup>, the Roadmap epigenomics project<sup>38</sup> as well as a range of other functional tools. ENCODE and Roadmap have assayed a large number of different cell types including keratinocyte and melanocyte primary cells, and, for a limited number of assays, melanoma cell lines; predicted functional activity in these cell types was given priority over cell types less likely to be involved in CMM risk. The summary results reported by HaploReg and RegulomeDB assign regions a putative function based on the combined results of multiple functional experiments and their position relative to known genes<sup>38,39</sup>. For example, ENCODE assigns the label of predicted enhancer to areas of open chromatin that overlaps a H3K4me1 signal, and binds transcription factors<sup>39</sup>. The Roadmap Epigenome uses a similar ranking system to ENCODE, and is summarized in the documentation for HaploReg<sup>37</sup>. For example, a weak enhancer will have only a weak H3K36me3 signal, while an active enhancer will have strong H3K36me3, H3K3me1 and H3K27ac signals. These labels are further divided into weak and strong depending on the quality of evidence. While these labels are predicted or putative, ENCODE reports that  $>50\%$  of predicted enhancers are confirmed by follow up assays<sup>39</sup>, and these serve as a useful guide for interrogating CMM associated SNPs. Results from these tools were followed up in more detail using the UCSC genome browser<sup>60</sup> to explore the ENCODE<sup>39</sup> and the Roadmap epigenomics project<sup>38</sup> data.

In addition, HaploReg uses genome-wide SNPs to estimate the background frequency of SNPs occurring in putative enhancer regions; this was used to test for enrichment in CMM-associated SNPs with an uncorrected binomial test threshold of  $P = 0.05^{37}$ .

The eQTL browser, the Genotype-Tissue Expression dataset (GTEx)<sup>55</sup>, and the Multiple Tissue Human Expression Resource (MuTHER<sup>43,88</sup>) were further interrogated to attempt to resolve potential genes influenced by disease associated SNPs. For these databases we report only *cis* results; details of cell types and definition of *cis* boundaries can be found in Supplementary Tables 7–9. The peak SNP for each locus, as well as other functionally interesting SNPs identified by HaploReg and RegulomeDB, were used to search listed eQTL databases. As the SNP coverage can differ for each database, where SNPs of interest were not present in the eQTL datasets we searched using high LD (>0.95) proxies. While priority was given to cell types more likely to be involved in CMM biology (e.g. sun-exposed skin from GTEx or skin from MuTHER) we reported eQTLs from other tissue types to highlight potential functional impact for identified SNPs.

Regional plots of  $-\log_{10}P$ -values were generated using LocusZoom<sup>89</sup>. Where pairwise linkage disequilibrium measures are given, these were estimated from the 379 European ancestry 1000 Genomes Phase 1 April 2012 samples using PLINK<sup>90</sup> or the `--hap-r2` command in VCFtools<sup>91</sup> unless otherwise indicated.

To test for any overlap with published GWAS association, results reported in the NHGRI catalog for reported loci were extracted on 24/07/2014 and cross checked against the Stage one meta-analysis results.

### Additional methods

Manhattan plots were generated in R based on scripts written by Stephen Turner (see URLs). Forest plots were generated using the R `rmeta` package<sup>92</sup>.

### Supplementary Material

Refer to Web version on PubMed Central for supplementary material.

### Authors

Matthew H. Law<sup>1,67</sup>, D. Timothy Bishop<sup>2,67</sup>, Jeffrey E. Lee<sup>#3</sup>, Myriam Brossard<sup>#4,5</sup>, Nicholas G. Martin<sup>6</sup>, Eric K. Moses<sup>7</sup>, Fengju Song<sup>8</sup>, Jennifer H. Barrett<sup>2</sup>, Rajiv Kumar<sup>9</sup>, Douglas F. Easton<sup>10</sup>, Paul D. P. Pharoah<sup>11</sup>, Anthony J. Swerdlow<sup>12,13</sup>, Katerina P. Kypreou<sup>14</sup>, John C. Taylor<sup>2</sup>, Mark Harland<sup>2</sup>, Juliette Randerson-Moor<sup>2</sup>, Lars A. Akslen<sup>15,16</sup>, Per A. Andresen<sup>17</sup>, Marie-Françoise Avril<sup>18</sup>, Esther Azizi<sup>19,20</sup>, Giovanna Bianchi Scarrà<sup>21,22</sup>, Kevin M. Brown<sup>23</sup>, Tadeusz Dębniak<sup>24</sup>, David L. Duffy<sup>6</sup>, David E. Elder<sup>25</sup>, Shenying Fang<sup>3</sup>, Eitan Friedman<sup>20</sup>, Pilar Galan<sup>26</sup>, Paola Ghorzo<sup>21,22</sup>, Elizabeth M. Gillanders<sup>27</sup>, Alisa M. Goldstein<sup>23</sup>, Nelleke A. Gruis<sup>28</sup>, Johan Hansson<sup>29</sup>, Per Helsing<sup>30</sup>, Marko Hoever<sup>31</sup>, Veronica Höiom<sup>29</sup>, Christian Ingvar<sup>32</sup>, Peter A. Kanetsky<sup>33</sup>, Wei V. Chen<sup>34</sup>, GenoMEL Consortium<sup>35</sup>, Essen-Heidelberg Investigators<sup>35</sup>, The SDH Study Group<sup>35</sup>, Q-MEGA and QTWIN

Investigators<sup>35</sup>, AMFS Investigators<sup>35</sup>, ATHENS Melanoma Study Group<sup>35</sup>, Maria Teresa Landi<sup>23</sup>, Julie Lang<sup>36</sup>, G. Mark Lathrop<sup>37</sup>, Jan Lubinski<sup>24</sup>, Rona M. Mackie<sup>38,39</sup>, Graham J. Mann<sup>40</sup>, Anders Molven<sup>16,41</sup>, Grant W. Montgomery<sup>42</sup>, Srdjan Novakovič, Håkan Olsson<sup>44,45</sup>, Susana Puig<sup>46,47</sup>, Joan Anton Puig-Butlle<sup>46,47</sup>, Abrar A. Qureshi<sup>48</sup>, Graham L. Radford-Smith<sup>49,50,51</sup>, Nienke van der Stoep<sup>52</sup>, Remco van Doorn<sup>28</sup>, David C. Whiteman<sup>53</sup>, Jamie E. Craig<sup>54</sup>, Dirk Schadendorf<sup>55,56</sup>, Lisa A. Simms<sup>49</sup>, Kathryn P. Burdon<sup>57</sup>, Dale R. Nyholt<sup>58,42</sup>, Karen A. Pooley<sup>10</sup>, Nicholas Orr<sup>59</sup>, Alexander J. Stratigos<sup>14</sup>, Anne E. Cust<sup>60</sup>, Sarah V. Ward<sup>7</sup>, Nicholas K. Hayward<sup>61</sup>, Jiali Han<sup>62,63</sup>, Hans-Joachim Schulze<sup>64</sup>, Alison M. Dunning<sup>11</sup>, Julia A. Newton Bishop<sup>2</sup>, Florence Demenais<sup>4,5</sup>, Christopher I. Amos<sup>65</sup>, Stuart MacGregor<sup>1,67</sup>, and Mark M. Iles<sup>2,67</sup>

## Affiliations

## Acknowledgements

Please see the Supplementary Note for acknowledgements.

## Author Affiliations

- <sup>1</sup>Statistical Genetics, QIMR Berghofer Medical Research Institute, Brisbane, Australia
- <sup>2</sup>Section of Epidemiology and Biostatistics, Leeds Institute of Cancer and Pathology, University of Leeds, Leeds, UK
- <sup>3</sup>Department of Surgical Oncology, The University of Texas MD Anderson Cancer Center, Houston, Texas, USA
- <sup>4</sup>Institut National de la Santé et de la Recherche Médicale (INSERM), UMR-946, Genetic Variation and Human Diseases Unit, Paris, France
- <sup>5</sup>Institut Universitaire d'Hématologie, Université Paris Diderot, Sorbonne Paris Cité, Paris, France
- <sup>6</sup>Genetic Epidemiology, QIMR Berghofer Medical Research Institute, Brisbane, Australia
- <sup>7</sup>Centre for Genetic Origins of Health and Disease, Faculty of Medicine, Dentistry and Health Sciences, The University of Western Australia, Western Australia, Australia
- <sup>8</sup>Departments of Epidemiology and Biostatistics, Key Laboratory of Cancer Prevention and Therapy, Tianjin, National Clinical Research Center of Cancer, Tianjin Medical University Cancer Institute and Hospital, Tianjin, P. R. China
- <sup>9</sup>Division of Molecular Genetic Epidemiology, German Cancer Research Center, Im Neuenheimer Feld 580, Heidelberg Germany
- <sup>10</sup>Centre for Cancer Genetic Epidemiology, Department of Public Health and Primary Care, University of Cambridge, Cambridge, UK
- <sup>11</sup>Centre for Cancer Genetic Epidemiology, Department of Oncology, University of Cambridge, Cambridge, UK
- <sup>12</sup>Division of Genetics and Epidemiology, The Institute of Cancer Research, London, UK
- <sup>13</sup>Division of Breast Cancer Research, The Institute of Cancer Research, London, UK
- <sup>14</sup>Department of Dermatology, University of Athens School of Medicine, Andreas Sygros Hospital, Athens, Greece

- <sup>15</sup>Centre for Cancer Biomarkers CCBIO, Department of Clinical Medicine, University of Bergen, Bergen, Norway
- <sup>16</sup>Department of Pathology, Haukeland University Hospital, Bergen, Norway
- <sup>17</sup>Department of Pathology, Molecular Pathology, Oslo University Hospital, Rikshospitalet, Oslo, Norway
- <sup>18</sup>Assistance Publique–Hôpitaux de Paris, Hôpital Cochin, Service de Dermatologie, Université Paris Descartes, Paris, France
- <sup>19</sup>Department of Dermatology, Sheba Medical Center, Tel Hashomer, Sackler Faculty of Medicine, Tel Aviv, Israel
- <sup>20</sup>Oncogenetics Unit, Sheba Medical Center, Tel Hashomer, Sackler Faculty of Medicine, Tel Aviv University, Tel Aviv, Israel
- <sup>21</sup>Department of Internal Medicine and Medical Specialties, University of Genoa, Genoa, Italy
- <sup>22</sup>Laboratory of Genetics of Rare Cancers, Istituto di ricovero e cura a carattere scientifico Azienda Ospedaliera Universitaria (IRCCS AOU) San Martino-IST Istituto Nazionale per la Ricerca sul Cancro, Genoa, Italy
- <sup>23</sup>Division of Cancer Epidemiology and Genetics, National Cancer Institute, National Institutes of Health, Bethesda, Maryland, USA
- <sup>24</sup>International Hereditary Cancer Center, Pomeranian Medical University, Szczecin, Poland
- <sup>25</sup>Department of Pathology and Laboratory Medicine, Perelman School of Medicine at the University of Pennsylvania, Philadelphia, Pennsylvania, USA
- <sup>26</sup>Université Paris 13, Equipe de Recherche en Epidémiologie Nutritionnelle (EREN), Centre de Recherche en Epidémiologie et Statistiques, Institut National de la Santé et de la Recherche Médicale (INSERM U1153), Institut National de la Recherche Agronomique (INRA U1125), Conservatoire National des Arts et Métiers, Communauté d'Université Sorbonne Paris Cité, F-93017 Bobigny, France
- <sup>27</sup>Inherited Disease Research Branch, National Human Genome Research Institute, National Institutes of Health, Baltimore, Maryland, USA
- <sup>28</sup>Department of Dermatology, Leiden University Medical Centre, Leiden, The Netherlands
- <sup>29</sup>Department of Oncology-Pathology, Karolinska Institutet, Karolinska University Hospital, Stockholm, Sweden
- <sup>30</sup>Department of Dermatology, Oslo University Hospital, Rikshospitalet, Oslo, Norway
- <sup>31</sup>Department of Surgical Oncology, Institute of Oncology Ljubljana, Ljubljana, Slovenia
- <sup>32</sup>Department of Surgery, Clinical Sciences, Lund University, Lund, Sweden
- <sup>33</sup>Department of Cancer Epidemiology, H. Lee Moffitt Cancer Center and Research Institute, Tampa, Florida, USA
- <sup>34</sup>Department of Genetics, The University of Texas MD Anderson Cancer Center, Houston, Texas, USA
- <sup>36</sup>Department of Medical Genetics, University of Glasgow, Glasgow, UK
- <sup>37</sup>McGill University and Genome Quebec Innovation Centre, Montreal, Canada
- <sup>38</sup>Department of Public Health, University of Glasgow, Glasgow UK
- <sup>39</sup>Department of Medical Genetics, University of Glasgow, Glasgow, UK
- <sup>40</sup>Centre for Cancer Research, University of Sydney at Westmead, Millennium Institute for Medical Research and Melanoma Institute Australia, Sydney, Australia



- <sup>41</sup>Gade Laboratory for Pathology, Department of Clinical Medicine, University of Bergen, Bergen, Norway
- <sup>42</sup>Molecular Epidemiology, QIMR Berghofer Medical Research Institute, Brisbane, Australia
- <sup>43</sup>Department of Molecular Diagnostics, Institute of Oncology Ljubljana, Ljubljana, Slovenia
- <sup>44</sup>Department of Oncology/Pathology, Clinical Sciences, Lund University, Lund; Sweden
- <sup>45</sup>Department of Cancer Epidemiology, Clinical Sciences, Lund University, Lund, Sweden
- <sup>46</sup>Melanoma Unit, Dermatology Department & Biochemistry and Molecular Genetics Departments, Hospital Clinic, Institut de Investigació Biomèdica August Pi Suñe, Universitat de Barcelona, Barcelona, Spain
- <sup>47</sup>Centro de Investigación Biomédica en Red (CIBER) de Enfermedades Raras, Instituto de Salud Carlos III, Barcelona, Spain
- <sup>48</sup>Department of Dermatology, The Warren Alpert Medical School of Brown University, Rhode Island, USA
- <sup>49</sup>Inflammatory Bowel Diseases, QIMR Berghofer Medical Research Institute, Brisbane, Australia
- <sup>50</sup>Department of Gastroenterology and Hepatology, Royal Brisbane & Women's Hospital, Brisbane, Australia
- <sup>51</sup>University of Queensland School of Medicine, Herston Campus, Brisbane, Australia
- <sup>52</sup>Department of Clinical Genetics, Center of Human and Clinical Genetics, Leiden University Medical Center, Leiden, The Netherlands
- <sup>53</sup>Cancer Control Group, QIMR Berghofer Medical Research Institute, Brisbane, Australia
- <sup>54</sup>Department of Ophthalmology, Flinders University, Adelaide, Australia
- <sup>55</sup>Department of Dermatology, University Hospital Essen, Essen, Germany
- <sup>56</sup>German Consortium Translational Cancer Research (DKTK), Heidelberg, Germany
- <sup>57</sup>Menzies Institute for Medical Research, University of Tasmania, Hobart, Tasmania, Australia
- <sup>58</sup>Institute of Health and Biomedical Innovation, Queensland University of Technology, Brisbane, Queensland, Australia
- <sup>59</sup>Breakthrough Breast Cancer Research Centre, The Institute of Cancer Research, London, UK
- <sup>60</sup>Cancer Epidemiology and Services Research, Sydney School of Public Health, The University of Sydney, Australia
- <sup>61</sup>Oncogenomics, QIMR Berghofer Medical Research Institute, Brisbane, Australia
- <sup>62</sup>Department of Epidemiology, Richard M. Fairbanks School of Public Health, Indiana University, Indianapolis, Indiana, USA
- <sup>63</sup>Melvin and Bren Simon Cancer Center, Indiana University, Indianapolis, Indiana, USA
- <sup>64</sup>Department of Dermatology, Fachklinik Hornheide, Institute for Tumors of the Skin at the University of Münster, Münster, Germany
- <sup>65</sup>Department of Community and Family Medicine, Geisel School of Medicine, Dartmouth College, Hanover, New Hampshire, USA

## Author Contributions

MMI led, designed and carried out the statistical analyses and wrote the manuscript. MHL led, designed and carried out the statistical analyses and wrote the manuscript. MH was involved in the Leeds genotyping design. JCT carried out statistical analyses. JR-M carried out genotyping and contributed to the interpretation of genotyping data. NvdS carried out genotyping and contributed to the interpretation of genotyping data. JANB led the GenoMEL consortium and contributed to study design. NAG was deputy lead of the consortium and contributed to study design. SMacG designed and led the overall study. NKH designed and led the overall study. DTB designed and led the overall study. JHB designed and led the overall study. JH supervised and carried out statistical analysis of the Harvard GWAS data. FS carried out statistical analysis of the Harvard GWAS data. AAQ carried out statistical analysis of the Harvard GWAS data. CIA led and carried out statistical analysis of the M.D. Anderson GWAS data. WVC contributed to the analysis and interpretation of the M.D. Anderson GWAS data. JEL contributed to the analysis and interpretation of the M.D. Anderson GWAS data. SF contributed to the analysis and interpretation of the M.D. Anderson GWAS data. FD led, designed and contributed to the sample collection, analysis and interpretation of the French MELARISK GWAS data and advised on the overall statistical analysis. MB contributed to the analysis and interpretation of the French MELARISK GWAS data. MFA led, designed and contributed to the sample collection of the French MELARISK GWAS data. GML led and contributed to the genotyping and interpretation of the French MELARISK GWAS data. RK led, and contributed to the sample collection and analysis for the Heidelberg dataset. DS led and contributed to the sample collection and analysis for the Heidelberg dataset. HJS contributed to the sample collection and analysis for the Heidelberg dataset. SVW led and contributed to the sample collection for the WAMHS study. EKM provided coordination and oversight for the WAMHS study. DCW led designed, and contributed to the sample collection for the SDH dataset. JEG led and designed the Glaucoma study. KPB contributed to the analysis and interpretation of the Glaucoma dataset. GLR-S led and contributed to the analysis and interpretation of the IBD dataset. LS contributed to the analysis and interpretation of the IBD dataset. GJM led and contributed to the sample collection, analysis and interpretation of the AMFS study. AEC contributed to the sample collection, analysis and interpretation of the AMFS study. DRN contributed to the sample collection and analysis of Q-MEGA, Endometriosis and QTWIN datasets. NGM led the sample collection and analysis of Q-MEGA and QTWIN datasets. GM led the sample collection and analysis of Endometriosis datasets, and contributed to the sample collection and analysis of Q-MEGA, Endometriosis and QTWIN datasets. DLD contributed to the sample collection and analysis of Q-MEGA, Endometriosis and QTWIN datasets. KMB contributed to the sample collection and analysis of Q-MEGA and QTWIN datasets. AJStratigos interpreted and contributed genotype data for the Athens Stage two dataset. KPK interpreted and contributed genotype data for the Athens Stage two dataset. AMG advised on statistical analysis. PAK advised on statistical analysis. EMG advised on statistical analysis. DEE contributed to the design of the GenoMEL GWAS. AJS interpreted and contributed genotype data for the Breakthrough Generations Study. NO interpreted and contributed genotype data for the Breakthrough Generations Study. LAA contributed to sample collection, analysis and interpretation of

GenoMEL datasets. PAA contributed to collection, analysis and interpretation of GenoMEL datasets. EA contributed to collection, analysis and interpretation of GenoMEL datasets. GBS contributed to collection, analysis and interpretation of GenoMEL datasets. TD contributed to collection, analysis and interpretation of GenoMEL datasets. EF contributed to sample collection, analysis and interpretation of GenoMEL datasets. PGh contributed to sample collection, analysis and interpretation of GenoMEL datasets. JH contributed to sample collection, analysis and interpretation of GenoMEL datasets. PHe contributed to sample collection, analysis and interpretation of GenoMEL datasets. MHo contributed to collection, analysis and interpretation of GenoMEL datasets. VH contributed to collection, analysis and interpretation of GenoMEL datasets. CIn contributed to collection, analysis and interpretation of GenoMEL datasets. MTL contributed to collection, analysis and interpretation of GenoMEL datasets. JLang contributed to collection, analysis and interpretation of GenoMEL datasets. RMM contributed to collection, analysis and interpretation of GenoMEL datasets. AM contributed to collection, analysis and interpretation of GenoMEL datasets. JLib. contributed to collection, analysis and interpretation of GenoMEL datasets. SN contributed to collection, analysis and interpretation of GenoMEL datasets. HO contributed to collection, analysis and interpretation of GenoMEL datasets. SP contributed to collection, analysis and interpretation of GenoMEL datasets. JAP-B contributed to collection, analysis and interpretation of GenoMEL datasets. RvD contributed to collection, analysis and interpretation of GenoMEL datasets. KAP interpreted and contributed genotype data for the Cambridge Stage two dataset. AMD interpreted and contributed genotype data for the Cambridge Stage two dataset. PDPP interpreted and contributed genotype data for the Cambridge Stage two dataset. DFE interpreted and contributed genotype data for the Cambridge Stage two dataset. PGal. contributed to collection, analysis and interpretation of the SU.VI.Max French control dataset. All authors provided critical review of the manuscript.

## References for main text

1. Holly EA, Aston DA, Cress RD, Ahn DK, Kristiansen JJ. Cutaneous melanoma in women. II. Phenotypic characteristics and other host-related factors. *Am J Epidemiol.* 1995; 141:934–42. [PubMed: 7741123]
2. Holly EA, Aston DA, Cress RD, Ahn DK, Kristiansen JJ. Cutaneous melanoma in women. I. Exposure to sunlight, ability to tan, and other risk factors related to ultraviolet light. *Am J Epidemiol.* 1995; 141:923–33. [PubMed: 7741122]
3. Naldi L, et al. Cutaneous malignant melanoma in women. Phenotypic characteristics, sun exposure, and hormonal factors: a case-control study from Italy. *Ann Epidemiol.* 2005; 15:545–50. [PubMed: 16029848]
4. Titus-Ernstoff L, et al. Pigmentary characteristics and moles in relation to melanoma risk. *Int J Cancer.* 2005; 116:144–9. [PubMed: 15761869]
5. Bataille V, et al. Risk of cutaneous melanoma in relation to the numbers, types and sites of naevi: a case-control study. *Br J Cancer.* 1996; 73:1605–11. [PubMed: 8664138]
6. Chang YM, et al. A pooled analysis of melanocytic nevus phenotype and the risk of cutaneous melanoma at different latitudes. *Int J Cancer.* 2009; 124:420–8. [PubMed: 18792098]
7. Cannon-Albright LA, Bishop DT, Goldgar C, Skolnick MH. Genetic predisposition to cancer. *Important Adv Oncol.* 1991:39–55. [PubMed: 1869281]
8. Brown KM, et al. Common sequence variants on 20q11.22 confer melanoma susceptibility. *Nat Genet.* 2008; 40:838–40. [PubMed: 18488026]

9. Bishop DT, et al. Genome-wide association study identifies three loci associated with melanoma risk. *Nat Genet.* 2009; 41:920–5. [PubMed: 19578364]
10. Amos CI, et al. Genome-wide association study identifies novel loci predisposing to cutaneous melanoma. *Hum Mol Genet.* 2011; 20:5012–23. [PubMed: 21926416]
11. Barrett JH, et al. Genome-wide association study identifies three new melanoma susceptibility loci. *Nat Genet.* 2011; 43:1108–13. [PubMed: 21983787]
12. Macgregor S, et al. Genome-wide association study identifies a new melanoma susceptibility locus at 1q21.3. *Nat Genet.* 2011; 43:1114–8. [PubMed: 21983785]
13. Iles MM, et al. A variant in FTO shows association with melanoma risk not due to BMI. *Nat Genet.* 2013; 45:428–32. 432e1. [PubMed: 23455637]
14. Gudbjartsson DF, et al. ASIP and TYR pigmentation variants associate with cutaneous melanoma and basal cell carcinoma. *Nat Genet.* 2008; 40:886–91. [PubMed: 18488027]
15. Antonopoulou K, et al. Updated field synopsis and systematic meta-analyses of genetic association studies in cutaneous melanoma: the MelGene database. *J Invest Dermatol.* 2015; 135:1074–9. [PubMed: 25407435]
16. Pena-Chilet M, et al. Genetic variants in PARP1 (rs3219090) and IRF4 (rs12203592) genes associated with melanoma susceptibility in a Spanish population. *BMC Cancer.* 2013; 13:160. [PubMed: 23537197]
17. Falchi M, et al. Genome-wide association study identifies variants at 9p21 and 22q13 associated with development of cutaneous nevi. *Nat Genet.* 2009; 41:915–9. [PubMed: 19578365]
18. Rafnar T, et al. Sequence variants at the TERT-CLPTM1L locus associate with many cancer types. *Nat Genet.* 2009; 41:221–7. [PubMed: 19151717]
19. Pooley KA, et al. No association between TERT-CLPTM1L single nucleotide polymorphism rs401681 and mean telomere length or cancer risk. *Cancer Epidemiol Biomarkers Prev.* 2010; 19:1862–5. [PubMed: 20570912]
20. Nan H, Qureshi AA, Prescott J, De Vivo I, Han J. Genetic variants in telomere-maintaining genes and skin cancer risk. *Hum Genet.* 2011; 129:247–53. [PubMed: 21116649]
21. Law MH, et al. Meta-analysis combining new and existing data sets confirms that the TERT-CLPTM1L locus influences melanoma risk. *J Invest Dermatol.* 2012; 132:485–7. [PubMed: 21993562]
22. Mocellin S, et al. Telomerase reverse transcriptase locus polymorphisms and cancer risk: a field synopsis and meta-analysis. *J Natl Cancer Inst.* 2012; 104:840–54. [PubMed: 22523397]
23. Gomez M, et al. PARP1 Is a TRF2-associated poly(ADP-ribose)polymerase and protects eroded telomeres. *Mol Biol Cell.* 2006; 17:1686–96. [PubMed: 16436506]
24. Derheimer FA, Kastan MB. Multiple roles of ATM in monitoring and maintaining DNA integrity. *FEBS Lett.* 2010; 584:3675–81. [PubMed: 20580718]
25. Bataille V, et al. Nevus size and number are associated with telomere length and represent potential markers of a decreased senescence in vivo. *Cancer Epidemiol Biomarkers Prev.* 2007; 16:1499–502. [PubMed: 17627017]
26. Han J, et al. A prospective study of telomere length and the risk of skin cancer. *J Invest Dermatol.* 2009; 129:415–21. [PubMed: 18668136]
27. Burke LS, et al. Telomere length and the risk of cutaneous malignant melanoma in melanoma-prone families with and without CDKN2A mutations. *PLoS One.* 2013; 8:e71121. [PubMed: 23990928]
28. Iles MM, et al. The effect on melanoma risk of genes previously associated with telomere length. *J Natl Cancer Inst.* 2014; 106
29. Barrett JH, et al. Fine mapping of genetic susceptibility loci for melanoma reveals a mixture of single variant and multiple variant regions. *Int J Cancer.* 2015; 136:1351–60. [PubMed: 25077817]
30. de Bakker PI, et al. Practical aspects of imputation-driven meta-analysis of genome-wide association studies. *Hum Mol Genet.* 2008; 17:R122–8. [PubMed: 18852200]
31. Miyake Y, et al. RPA-like mammalian Ctc1-Stn1-Ten1 complex binds to single-stranded DNA and protects telomeres independently of the Pot1 pathway. *Mol Cell.* 2009; 36:193–206. [PubMed: 19854130]

32. van Steensel B, de Lange T. Control of telomere length by the human telomeric protein TRF1. *Nature*. 1997; 385:740–3. [PubMed: 9034193]
33. Robles-Espinoza CD, et al. POT1 loss-of-function variants predispose to familial melanoma. *Nat Genet*. 2014; 46:478–81. [PubMed: 24686849]
34. Shi J, et al. Rare missense variants in POT1 predispose to familial cutaneous malignant melanoma. *Nat Genet*. 2014; 46:482–6. [PubMed: 24686846]
35. Codd V, et al. Identification of seven loci affecting mean telomere length and their association with disease. *Nat Genet*. 2013; 45:422–7. 427e1–2. [PubMed: 23535734]
36. Yang J, Lee SH, Goddard ME, Visscher PM. GCTA: a tool for genome-wide complex trait analysis. *Am J Hum Genet*. 2011; 88:76–82. [PubMed: 21167468]
37. Ward LD, Kellis M. HaploReg: a resource for exploring chromatin states, conservation, and regulatory motif alterations within sets of genetically linked variants. *Nucleic Acids Res*. 2012; 40:D930–4. [PubMed: 22064851]
38. Bernstein BE, et al. The NIH Roadmap Epigenomics Mapping Consortium. *Nat Biotechnol*. 2010; 28:1045–8. [PubMed: 20944595]
39. Consortium, E.P. An integrated encyclopedia of DNA elements in the human genome. *Nature*. 2012; 489:57–74. [PubMed: 22955616]
40. Boyle AP, et al. Annotation of functional variation in personal genomes using RegulomeDB. *Genome Res*. 2012; 22:1790–7. [PubMed: 22955989]
41. Schadt EE, et al. Mapping the genetic architecture of gene expression in human liver. *PLoS Biol*. 2008; 6:e107. [PubMed: 18462017]
42. Innocenti F, et al. Identification, replication, and functional fine-mapping of expression quantitative trait loci in primary human liver tissue. *PLoS Genet*. 2011; 7:e1002078. [PubMed: 21637794]
43. Grundberg E, et al. Mapping cis- and trans-regulatory effects across multiple tissues in twins. *Nat Genet*. 2012; 44:1084–9. [PubMed: 22941192]
44. Gajjar K, Martin-Hirsch PL, Martin FL. CYP1B1 and hormone-induced cancer. *Cancer Lett*. 2012; 324:13–30. [PubMed: 22561558]
45. Muthusamy V, et al. Epigenetic silencing of novel tumor suppressors in malignant melanoma. *Cancer Res*. 2006; 66:11187–93. [PubMed: 17145863]
46. Shen M, et al. Quantitative assessment of the influence of CYP1B1 polymorphisms and head and neck squamous cell carcinoma risk. *Tumour Biol*. 2014; 35:3891–7. [PubMed: 24343338]
47. Stoilov I, Akarsu AN, Sarfarazi M. Identification of three different truncating mutations in cytochrome P4501B1 (CYP1B1) as the principal cause of primary congenital glaucoma (Buphthalmos) in families linked to the GLC3A locus on chromosome 2p21. *Hum Mol Genet*. 1997; 6:641–7. [PubMed: 9097971]
48. Arragain S, et al. Identification of eukaryotic and prokaryotic methylthiotransferase for biosynthesis of 2-methylthio-N6-threonylcarbamoyladenine in tRNA. *J Biol Chem*. 2010; 285:28425–33. [PubMed: 20584901]
49. Brambillasca S, et al. CDK5 regulatory subunit-associated protein 1-like 1 (CDKAL1) is a tail-anchored protein in the endoplasmic reticulum (ER) of insulinoma cells. *J Biol Chem*. 2012; 287:41808–19. [PubMed: 23048041]
50. Praetorius C, et al. A polymorphism in IRF4 affects human pigmentation through a tyrosinase-dependent MITF/TFAP2A pathway. *Cell*. 2013; 155:1022–33. [PubMed: 24267888]
51. Sulem P, et al. Genetic determinants of hair, eye and skin pigmentation in Europeans. *Nat Genet*. 2007; 39:1443–52. [PubMed: 17952075]
52. Han J, et al. A genome-wide association study identifies novel alleles associated with hair color and skin pigmentation. *PLoS Genet*. 2008; 4:e1000074. [PubMed: 18483556]
53. Duffy DL, et al. IRF4 variants have age-specific effects on nevus count and predispose to melanoma. *Am J Hum Genet*. 2010; 87:6–16. [PubMed: 20602913]
54. Zhang M, et al. Genome-wide association studies identify several new loci associated with pigmentation traits and skin cancer risk in European Americans. *Hum Mol Genet*. 2013; 22:2948–59. [PubMed: 23548203]

55. Consortium, G.T. The Genotype-Tissue Expression (GTEx) project. *Nat Genet.* 2013; 45:580–5. [PubMed: 23715323]
56. Consortium, G.T. Human genomics. The Genotype-Tissue Expression (GTEx) pilot analysis: multitissue gene regulation in humans. *Science.* 2015; 348:648–60. [PubMed: 25954001]
57. Persson S, et al. Diversity of the protein disulfide isomerase family: identification of breast tumor induced Hag2 and Hag3 as novel members of the protein family. *Mol Phylogenet Evol.* 2005; 36:734–40. [PubMed: 15935701]
58. Fletcher GC, et al. hAG-2 and hAG-3, human homologues of genes involved in differentiation, are associated with oestrogen receptor-positive breast tumours and interact with metastasis gene C4.4a and dystroglycan. *Br J Cancer.* 2003; 88:579–85. [PubMed: 12592373]
59. King ER, et al. The anterior gradient homolog 3 (AGR3) gene is associated with differentiation and survival in ovarian cancer. *Am J Surg Pathol.* 2011; 35:904–12. [PubMed: 21451362]
60. Kent WJ, et al. The human genome browser at UCSC. *Genome Research.* 2002; 12:996–1006. [PubMed: 12045153]
61. Masutani C, et al. Purification and cloning of a nucleotide excision repair complex involving the xeroderma pigmentosum group C protein and a human homologue of yeast RAD23. *EMBO J.* 1994; 13:1831–43. [PubMed: 8168482]
62. Xia Y, et al. TAL2, a helix-loop-helix gene activated by the (7;9)(q34;q32) translocation in human T-cell leukemia. *Proc Natl Acad Sci U S A.* 1991; 88:11416–20. [PubMed: 1763056]
63. Wong CW, et al. Kruppel-like transcription factor 4 contributes to maintenance of telomerase activity in stem cells. *Stem Cells.* 2010; 28:1510–7. [PubMed: 20629177]
64. Hoffmeyer K, et al. Wnt/beta-catenin signaling regulates telomerase in stem cells and cancer cells. *Science.* 2012; 336:1549–54. [PubMed: 22723415]
65. Teerlink C, et al. A unique genome-wide association analysis in extended Utah high-risk pedigrees identifies a novel melanoma risk variant on chromosome arm 10q. *Hum Genet.* 2012; 131:77–85. [PubMed: 21706340]
66. Vizekeleti L, et al. The role of CCND1 alterations during the progression of cutaneous malignant melanoma. *Tumour Biol.* 2012; 33:2189–99. [PubMed: 23001925]
67. Young RJ, et al. Loss of CDKN2A expression is a frequent event in primary invasive melanoma and correlates with sensitivity to the CDK4/6 inhibitor PD0332991 in melanoma cell lines. *Pigment Cell Melanoma Res.* 2014; 27:590–600. [PubMed: 24495407]
68. French JD, et al. Functional variants at the 11q13 risk locus for breast cancer regulate cyclin D1 expression through long-range enhancers. *Am J Hum Genet.* 2013; 92:489–503. [PubMed: 23540573]
69. Duffy DL, et al. A three-single-nucleotide polymorphism haplotype in intron 1 of OCA2 explains most human eye-color variation. *Am J Hum Genet.* 2007; 80:241–52. [PubMed: 17236130]
70. Ruiz Y, et al. Further development of forensic eye color predictive tests. *Forensic Sci Int Genet.* 2013; 7:28–40. [PubMed: 22709892]

## Methods only references

71. Price AL, et al. Principal components analysis corrects for stratification in genome-wide association studies. *Nat Genet.* 2006; 38:904–9. [PubMed: 16862161]
72. Howie BN, Donnelly P, Marchini J. A flexible and accurate genotype imputation method for the next generation of genome-wide association studies. *PLoS Genet.* 2009; 5:e1000529. [PubMed: 19543373]
73. Marchini J, Howie B. Genotype imputation for genome-wide association studies. *Nat Rev Genet.* 2010; 11:499–511. [PubMed: 20517342]
74. Li Y, Willer CJ, Ding J, Scheet P, Abecasis GR. MaCH: using sequence and genotype data to estimate haplotypes and unobserved genotypes. *Genet Epidemiol.* 2010; 34:816–34. [PubMed: 21058334]
75. Li Y, Willer C, Sanna S, Abecasis G. Genotype imputation. *Annu Rev Genomics Hum Genet.* 2009; 10:387–406. [PubMed: 19715440]

76. Howie B, Fuchsberger C, Stephens M, Marchini J, Abecasis GR. Fast and accurate genotype imputation in genome-wide association studies through pre-phasing. *Nat Genet.* 2012; 44:955–9. [PubMed: 22820512]
77. Genomes Project, C. et al. A map of human genome variation from population-scale sequencing. *Nature.* 2010; 467:1061–73. [PubMed: 20981092]
78. Marchini J, Howie B, Myers S, McVean G, Donnelly P. A new multipoint method for genome-wide association studies by imputation of genotypes. *Nat Genet.* 2007; 39:906–13. [PubMed: 17572673]
79. Higgins JP, Thompson SG. Quantifying heterogeneity in a meta-analysis. *Stat Med.* 2002; 21:1539–58. [PubMed: 12111919]
80. DerSimonian R, Laird N. Meta-analysis in clinical trials. *Control Clin Trials.* 1986; 7:177–88. [PubMed: 3802833]
81. Magi R, Morris AP. GWAMA: software for genome-wide association meta-analysis. *BMC Bioinformatics.* 2010; 11:288. [PubMed: 20509871]
82. Gabriel S, Ziaugra L, Tabbaa D. SNP genotyping using the Sequenom MassARRAY iPLEX platform. *Curr Protoc Hum Genet.* 2009:12. Chapter 2, Unit 2. [PubMed: 19170031]
83. Cho E, Rosner BA, Feskanich D, Colditz GA. Risk factors and individual probabilities of melanoma for whites. *J Clin Oncol.* 2005; 23:2669–75. [PubMed: 15837981]
84. Newton-Bishop JA, et al. Melanocytic nevi, nevus genes, and melanoma risk in a large case-control study in the United Kingdom. *Cancer Epidemiol Biomarkers Prev.* 2010; 19:2043–54. [PubMed: 20647408]
85. Newton-Bishop JA, et al. Relationship between sun exposure and melanoma risk for tumours in different body sites in a large case-control study in a temperate climate. *Eur J Cancer.* 2011; 47:732–41. [PubMed: 21084183]
86. Newton-Bishop JA, et al. Serum 25-hydroxyvitamin D3 levels are associated with breslow thickness at presentation and survival from melanoma. *J Clin Oncol.* 2009; 27:5439–44. [PubMed: 19770375]
87. Edwards SL, Beesley J, French JD, Dunning AM. Beyond GWASs: illuminating the dark road from association to function. *Am J Hum Genet.* 2013; 93:779–97. [PubMed: 24210251]
88. Nica AC, et al. The architecture of gene regulatory variation across multiple human tissues: the MuTHER study. *PLoS Genet.* 2011; 7:e1002003. [PubMed: 21304890]
89. Pruim RJ, et al. LocusZoom: regional visualization of genome-wide association scan results. *Bioinformatics.* 2010; 26:2336–7. [PubMed: 20634204]
90. Purcell S, et al. PLINK: a tool set for whole-genome association and population-based linkage analyses. *Am J Hum Genet.* 2007; 81:559–75. [PubMed: 17701901]
91. Danecek P, et al. The variant call format and VCFtools. *Bioinformatics.* 2011; 27:2156–8. [PubMed: 21653522]
92. Lumley, T. *rmeta: Meta-analysis.* R package version 2.16 edn. 2012.
93. Li MX, Yeung JM, Cherny SS, Sham PC. Evaluating the effective numbers of independent tests and significant p-value thresholds in commercial genotyping arrays and public imputation reference datasets. *Hum Genet.* 2012; 131:747–56. [PubMed: 22143225]

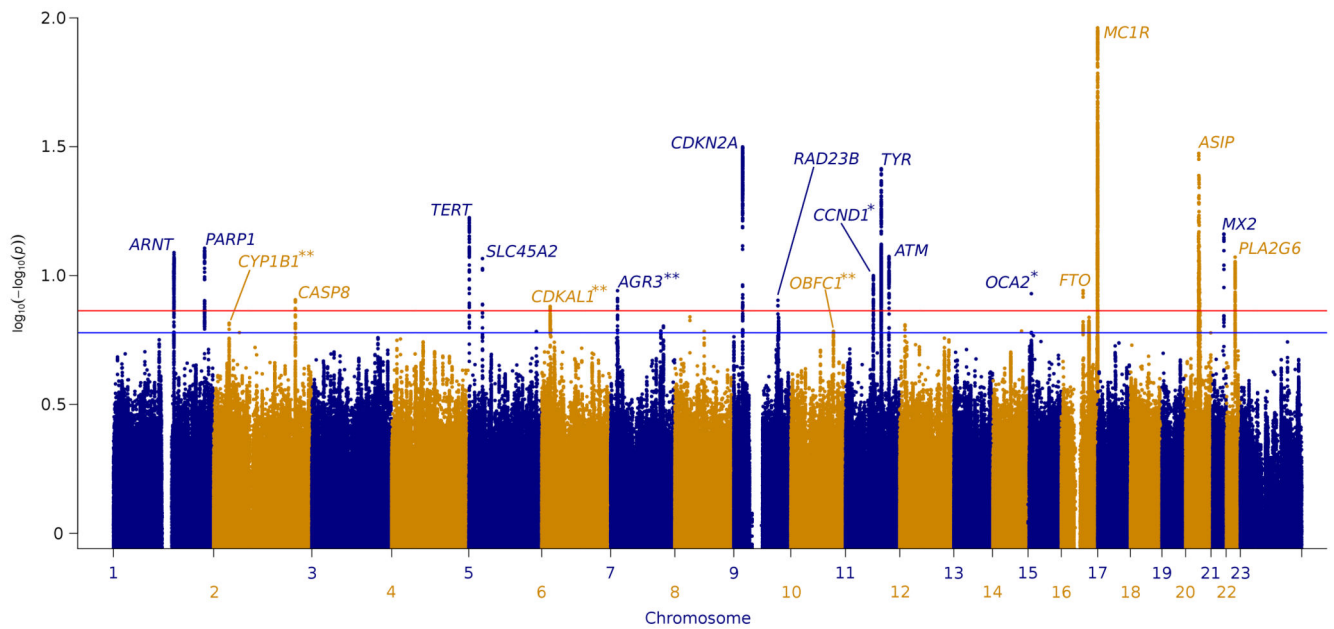


**Figure 1. Manhattan plot of the Stage one meta-analysis of GWAS of CMM from Europe, the USA and Australia**

The  $P_{fixed}$  Stage one value for all SNPs present in at least two studies have been plotted using a  $\log_{10}(-\log_{10}(p))$  to truncate the strong signals at *MC1R* ( $P < 10^{-92}$ ) on chromosome 16 and *CDKN2A* ( $P < 10^{-31}$ ) on chromosome 9. The total Stage one meta-analysis included 11 CMM GWAS, totaling 12,874 cases and 23,203 controls.  $P < 5 \times 10^{-8}$  (genome-wide significance) and  $P < 1 \times 10^{-6}$  are indicated by a red and a blue line respectively. 18 loci reached genome-wide significance in Stage one. The 2 newly-confirmed loci 11q13.3 (*CCND1*) and 15q13.1 (*HERC2/OCA2*) are indicated by \* and the 5 novel loci 2p22.2, 6p22.3, 7p21.1, 9q31.2 and 10q24.33 are highlighted by \*\*. 2p22.2 (*RMDN2/CYP1B1*) and 10q24.33 (*OBFC1*) were genome-wide significant only in the Overall meta-analysis (Supplementary Table 3).



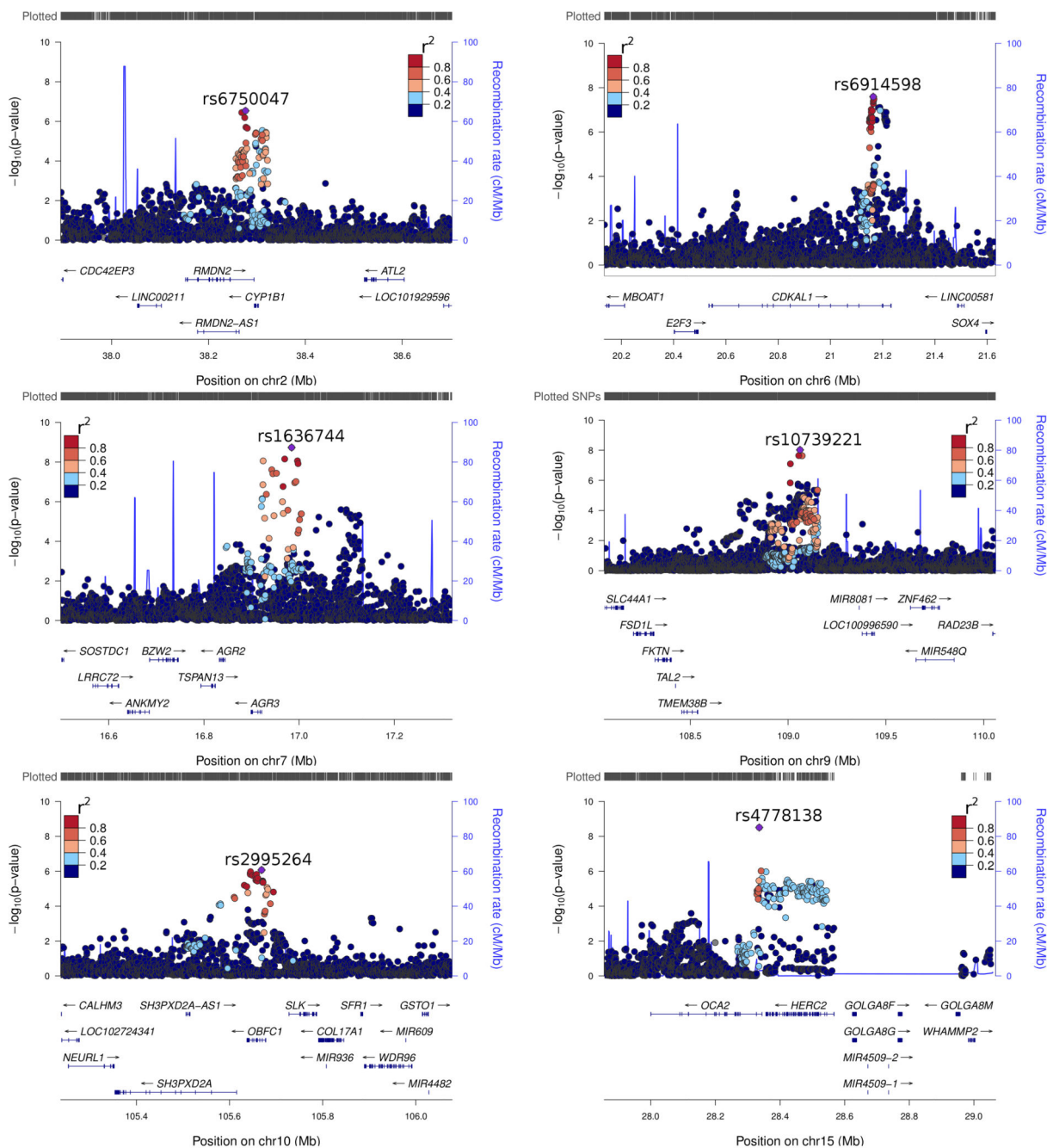


**Figure 2. Regional association plots for novel genome-wide significant loci 2p22.2, 6p22.3, 7p21.1, 9q31.2, 10q24.33 and the newly-confirmed region, 15q13.1 (*OCA2*)**

The negative  $\log_{10}$  of  $P_{fixed}$  values for SNPs from the Stage one meta-analysis of 12,874 cases and 23,203 controls have been plotted against their genomic position (Mb) using LocusZoom<sup>89</sup>. The rs ID is listed for the peak SNP in each region (purple diamond). The  $P$ -values and effect sizes for listed SNPs can be found in Supplementary Table 3. For the remaining SNPs the color indicates linkage disequilibrium  $r^2$  with the peak SNP. Note *FAM82A1*'s alternative gene ID is *RMND2*. Neither rs2995264 in 10q24.33 nor rs6750047

in 2p22.2 are genome-wide significant in Stage one, but reach this in the Overall meta-analysis. The plot for 11q13.3 (*CCND1*) can be found in Supplementary Figure 4.

**Table 1**  
**Genome-wide significant results from a two-stage meta-analysis of GWAS of CMM from Europe, the USA and Australia**

For each region we report the chromosomal location, nearest gene, and any other promising candidate gene in brackets for the top SNP. We also report the 1000 Genomes European population minor allele frequency (MAF) and minimum imputation quality across all studies (min INFO). The Stage one meta-analysis field reports the effect size estimate (beta) and *P*-value for the minor allele from the meta-analysis of 11 CMM GWAS, totaling 12,874 cases and 23,203 controls. Following their genotyping in three additional datasets (total 3,116 cases and 3,206 controls) we provide the Stage two meta-analysis results. Finally we provide the Overall meta-analysis of all available data. The results for the top SNP in each region that reached  $P < 1 \times 10^{-6}$  in Stage one and so was genotyped in Stage two, per study results and evidence of heterogeneity of effect estimates across studies ( $I^2$ ) can be found in Supplementary Table 3. Where  $I^2$  values were below 31% fixed effects meta-analysis was used, otherwise random effects, and all genome-wide significant SNPs had low heterogeneity ( $I^2 < 31\%$ ) in both Stage one and Overall. Regions previously confirmed as associated with melanoma (e.g. *MC1R*) are not shown.

SNP	Region	Gene	Minor Allele:MAF (min INFO)	Stage one meta-analysis		Stage two meta-analysis		Overall meta-analysis	
				Beta (P)		Beta (P)		Beta (P)	
rs6750047	2p22.2	<i>RMDN2</i> ( <i>CYP11B1</i> )	A:0.43 (0.96)	0.088 ( $2.9 \times 10^{-7}$ )	0.113 ( $6.0 \times 10^{-3}$ )	0.092 ( $7.0 \times 10^{-9}$ )			
rs6914598	6p22.3	<i>CDKALI</i>	C:0.32 (0.88)	0.11 ( $2.6 \times 10^{-8}$ )	0.037 (0.63)	0.10 ( $3.5 \times 10^{-8}$ )*			
rs1636744	7p21.1	<i>AGR3</i>	T:0.40 (0.96)	0.11 ( $1.8 \times 10^{-9}$ )	0.032 (0.38)	0.091 ( $7.1 \times 10^{-9}$ )			
rs10739221	9q31.2	<i>TMEM38B</i> ( <i>RAD23B</i> , <i>TAL2</i> )	T:0.24 (0.94)	0.12 ( $9.6 \times 10^{-9}$ )	0.145 ( $1.7 \times 10^{-3}$ )	0.12 ( $7.1 \times 10^{-11}$ )			
rs2995264	10q24.33	<i>OBFC1</i>	G:0.088 (0.94)	0.14 ( $8.5 \times 10^{-7}$ )	0.206 (0.088)	0.16 ( $2.2 \times 10^{-9}$ )			
rs498136	11q13.3	<i>CCND1</i>	A:0.32 (0.97)	0.12 ( $1.0 \times 10^{-10}$ )	0.124 ( $4.0 \times 10^{-3}$ )	0.12 ( $1.5 \times 10^{-12}$ )			
rs4778138	15q13.1	<i>OCA2</i>	G:0.16 (0.82)	-0.18 ( $3.1 \times 10^{-9}$ )	-0.156 ( $1.7 \times 10^{-3}$ )	-0.17 ( $2.2 \times 10^{-11}$ )			

\* Not genome-wide significant given after formal multiple testing correction e.g.  $P < 3.06 \times 10^{-8}$  as in Li et al. (2012)<sup>93</sup>.